ORIGINAL PAPER

Quantification of tidal watertable overheight in a coastal unconfined aquifer

Zhiyao Song · Ling Li · Peter Nielsen · David Lockington

Abstract   Tidal watertable fluctuations in a coastal aquifer are driven by tides on a moving boundary that varies with the beach slope. Based on a linearised one-dimensional Boussinesq model, tidal signals in the aquifer are analysed, focusing on the watertable overheight induced by the moving-boundary condition. The watertable overheight is an important parameter related to the estimation of submarine groundwater discharge (SGD). This note presents a new analytical approach to solving the Boussinesq equation with the Fourier-series expansion. Moreover, it is proved that the asymptote of watertable overheight normalised by the tidal amplitude is unit as a controlling parameter (ε_0), combining the aquifer properties and tidal frequency, approaches infinity. Physically, this condition represents beaches of very low drainage capacity.

Keywords   Boussinesq equation · Fourier series · Moving boundary · Tidal water-table fluctuation

1 Introduction

Under the action of tides on sloping sandy beaches, coastal groundwater levels rise, resulting in watertable overheight above the mean sea level (MSL in Fig. 1). Generally, watertable overheight is defined as the difference between the time-averaged watertable and MSL for far inland in the absence of regional groundwater flow. The generation of watertable overheight is attributed to the formation of a seepage face on the

Z. Song (✉)
State Key Laboratory of Hydrology-Water Resources and Hydraulic Engineering, Ocean College,
Hohai University, Nanjing 210098, P. R. China
e-mail: zhiyaosong@vip.sohu.com

Z. Song · L. Li
Center for Eco-Environmental Modelling,
Hohai University, Nanjing 210098, P. R. China
e-mail: l.li@uq.edu.au

L. Li · P. Nielsen · D. Lockington
School of Engineering, The University of Queensland, St. Lucia, QLD 4072, Australia
e-mail: p.nielsen@uq.edu.au

D. Lockington
e-mail: d.lockington@uq.edu.au

Fig. 1 Schematic diagram of tidal watertable fluctuations in a coastal aquifer
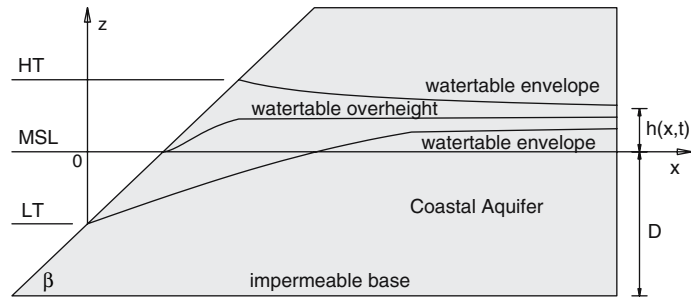
beach, giving rise to a moving-boundary condition due to the slope and nonlinearity of tidal propagation (e.g., [1–4]). While the seepage-face formation is not well understood, the latter two mechanisms have been quantified previously.

Using a perturbation technique, Parlange et al. [2] derived an approximate analytical solution to the nonlinear Boussinesq equation. The solution demonstrates the nonlinear effects on tidal propagation in the aquifer, which are manifested as generations of sub-harmonics and watertable overheight. Nielsen [3] and Li et al. [4] examined the moving (sloping) boundary effects. Although different approaches were adopted to deal with the moving-boundary conditions, both studies were based on perturbation solutions with the same dimensionless perturbation parameter, $\varepsilon_0 = A \cot(\beta) \sqrt{\frac{n_e \omega}{2KD}}$; (here A and ω are tidal amplitude [L] and frequency [radT^{-1}], respectively; β is the beach angle [rad]; K, n_e and D are the hydraulic conductivity [LT^{-1}], effective porosity and mean thickness of the aquifer [L], respectively). The solutions provide predictions of the watertable overheight within the constraint of $\varepsilon_0 < 1$.

Tide-induced watertable overheight is an important parameter, controlling the seaward boundary conditions for regional groundwater flow in coastal aquifers. Quantification of the watertable overheight is an essential task in estimating the submarine groundwater discharge (SGD) and associated chemical input to the ocean. The effects of SGD on the coastal marine eco-system have been recognised in many recent studies [5–9].

As discussed above, previous analytical studies of moving-boundary effects on watertable overheight are limited by the condition of $\varepsilon_0 < 1$. At natural coasts, this condition may be violated due to, for example, small beach slopes. In the present study, we adopt a new approach to the problem. The derived solution applies for $\varepsilon_0 > 1$ in theory; however, the solution with finite terms in practical applications deteriorates as ε_0 becomes larger than 3·0, which is due to the accuracy limitation in determining the coefficients of the truncated solution series. However, based on the new approach, we can prove that the asymptote of the tidal watertable overheight equals the tidal amplitude as ε_0 approaches infinity. This result was obtained only numerically by Callaghan and Nielsen [10].

2 Problem set-up

We consider one-dimensional groundwater flow in an unconfined coastal aquifer with a horizontal impermeable base to be homogeneous, isothermal and incompressible. Other assumptions are: (1) the aquifer is relatively shallow (i.e., small value of $n_e \omega D / K$); (2) the ratio of the tidal amplitude to the aquifer thickness is small; this is a valid assumption in most cases; (3) the extent of seepage face at the beach is negligible compared with the length of tidal excursion; and (4) the regional groundwater-head gradient (flow) is small and negligible.

This flow is often modelled by a linearised Boussinesq equation (e.g., [11, Chapter 2], [3, 4]),

$$\frac{\partial h}{\partial t} = \frac{KD}{n_e} \frac{\partial^2 h}{\partial x^2}, \tag{1}$$

where x[L] is the horizontal inland coordinate normal to the coastline; t [T] is time; $h(x,t)$ [L] is the watertable height from the mid-tidal sea level (Fig. 1); D is the mean aquifer thickness, K is the saturated hydraulic conductivity, and n_e is the effective porosity (all assumed to be constants).

In Fig. 1, HT and LT are the abbreviation for high tide, and low tide, respectively; two watertable envelopes represent the maximum and minimum watertable fluctuation along the x-direction.

At the coast, the moving-boundary condition is given by

$$h(x_0(t),t) = \eta(t) = A\cos(\omega t) \quad \text{and} \quad x_0(t) = \cot(\beta)(A + \eta(t)), \tag{2a}$$

where $x_0(t)$ is the x-coordinate of the moving boundary; the origin of the x-coordinate is located at the intersection between the low-tidal sea level (LT) and the beach surface as shown in Fig. 1; β is the slope of the beach; $\eta(t)$ represents tidal oscillations of the mean sea level; A is the tidal amplitude; and ω is the tidal frequency.

Far inland ($x \to \infty$), the gradient of h is taken to be zero (the tidal effects are diminished), i.e.,

$$\left.\frac{\partial h}{\partial x}\right|_{x\to\infty} = 0. \tag{2b}$$

Here we consider only the tidal effects.

For the purpose of simplicity and generality, the following nondimensional variables are introduced:

$$X = x/L, \quad H = h/A \quad \text{and} \quad T = \omega t, \tag{3}$$

where $L = \sqrt{\frac{KD}{n_e\omega}}$ represents a decay length scale of watertable fluctuations. Substituting (3) to (1) gives

$$\frac{\partial H}{\partial T} = \frac{\partial^2 H}{\partial X^2} \tag{4}$$

with the corresponding boundary conditions as follows

$$H(X_0(T),T) = \cos(T) \quad \text{and} \quad X_0(T) = \varepsilon(1 + \cos(T)), \tag{5a}$$

$$\left.\frac{\partial H}{\partial X}\right|_{X\to\infty} = 0, \tag{5b}$$

where $\varepsilon = A\cot(\beta)/L = A\cot(\beta)\sqrt{\frac{n_e\omega}{KD}}$ is a dimensionless parameter, combining all participating dimensional parameters. Note that this parameter is related to the perturbation variable (ε_0) used by Nielsen [3] and Li et al. [4] simply as $\varepsilon = \sqrt{2}\varepsilon_0$. Note that we are seeking a periodic solution to (4) and hence do not need to specify the initial condition with the following analytical approach.

The governing Eq. 4 subject to (5b) has a general solution of the following form

$$H(X,T) = A_0(\varepsilon) + \sum_{n=1}^{\infty} \exp(-k_n X)(A_n(\varepsilon)\cos(nT - k_n X) + B_n(\varepsilon)\sin(nT - k_n X)), \tag{6}$$

where $k_n = \sqrt{n/2}\,\varepsilon$ is the wave number for wave frequency n; $A_0(\varepsilon)$, $A_n(\varepsilon)$ and $B_n(\varepsilon)$ are dimensionless coefficients depending on ε, $A_0(\varepsilon)$ represents the watertable overheight. The coefficients $A_n(\varepsilon)$ and $B_n(\varepsilon)$ are to be determined by matching the moving-boundary condition (5a), that is

$$A_0(\varepsilon) + \sum_{n=1}^{\infty}\left(A_n(\varepsilon)f_n(\varepsilon,T) + B_n(\varepsilon)g_n(\varepsilon,T)\right) = \cos(T), \tag{7a}$$

where

$$f_n(\varepsilon,T) = \exp\left\{-\sqrt{n/2}\,\varepsilon(1 + \cos(T))\right\}\cos\left\{nT - \sqrt{n/2}\,\varepsilon(1 + \cos(T))\right\} \tag{7b}$$

and

$$g_n(\varepsilon,T) = \exp\left\{-\sqrt{n/2}\,\varepsilon(1 + \cos(T))\right\}\sin\left\{nT - \sqrt{n/2}\,\varepsilon(1 + \cos(T))\right\}. \tag{7c}$$

3 Fourier-series expansion

Under the condition $\varepsilon_0 < 1$, f_n and g_n can be expanded into power series of $\varepsilon/\sqrt{2}$ (ε_0), which leads to an approximate solution as obtained by Nielsen [3]. Here we adopt a new approach to solving (7), which does not require this condition.

Since $f_n(\varepsilon, T)$ and $g_n(\varepsilon, T)$ are periodic functions, we can expand them into Fourier series so that [12, Chapter 19]

$$f_n(\varepsilon, T) = \frac{a_{n,0}(\varepsilon)}{2} + \sum_{l=1}^{\infty} \left(a_{n,l}(\varepsilon) \cos(lT) + b_{n,l}(\varepsilon) \sin(lT) \right), \tag{8}$$

$$g_n(\varepsilon, T) = \frac{c_{n,0}(\varepsilon)}{2} + \sum_{l=1}^{\infty} \left(c_{n,l}(\varepsilon) \cos(lT) + d_{n,l}(\varepsilon) \sin(lT) \right) \tag{9}$$

with the Fourier coefficients determined as follows,

$$a_{n,l}(\varepsilon) = \frac{1}{\pi} \int_0^{2\pi} f_n(\varepsilon, T) \cos(lT) \mathrm{d}T, \tag{10a}$$

$$b_{n,l}(\varepsilon) = \frac{1}{\pi} \int_0^{2\pi} f_n(\varepsilon, T) \sin(lT) \mathrm{d}T, \tag{10b}$$

$$c_{n,l}(\varepsilon) = \frac{1}{\pi} \int_0^{2\pi} g_n(\varepsilon, T) \cos(lT) \mathrm{d}T, \tag{10c}$$

$$d_{n,l}(\varepsilon) = \frac{1}{\pi} \int_0^{2\pi} g_n(\varepsilon, T) \sin(lT) \mathrm{d}T. \tag{10d}$$

Substituting (8) and (9) in the right-hand side of (7) and equating the corresponding terms of each side of (7), we have

(1) for $l = 0$:

$$A_0(\varepsilon) + \frac{1}{2} \sum_{n=1}^{\infty} \left(a_{n,0}(\varepsilon) A_n(\varepsilon) + c_{n,0}(\varepsilon) B_n(\varepsilon) \right) = 0, \tag{11}$$

(2) for $\cos(lT)$ $(l \neq 0)$:

$$\sum_{n=1}^{\infty} \left(a_{n,l}(\varepsilon) A_n(\varepsilon) + c_{n,l}(\varepsilon) B_n(\varepsilon) \right) = \begin{cases} 1 & l = 1, \\ 0 & l \neq 1, \end{cases} \tag{12}$$

(3) for $\sin(lT)$ $(l \neq 0)$:

$$\sum_{n=1}^{\infty} \left(b_{n,l}(\varepsilon) A_n(\varepsilon) + d_{n,l}(\varepsilon) B_n(\varepsilon) \right) = 0, \quad l \geq 1. \tag{13}$$

In practical applications, for specified finite values of ε we can take finite terms to match the boundary condition in (7a) approximately, e.g., $n = 1, \ldots, m$. Subsequently a finite Fourier-series expansion ($l = 1, \ldots, j$) is undertaken for each term. Thus we obtain a set of linear algebraic equations ($2 \times m$) from (12) and (13), which can be solved using, for example, the Gauss–Seidel method to determine the coefficient A_n and B_n ($n = 1, \ldots, m$). The watertable overheight can then be calculated according to (11).

Results of calculated watertable overheight for a range of ε-values are shown in Table 1. For the sake of comparison, we also list in this table the numerical ("exact") results of the watertable overheight obtained

Table 1 Comparison of the watertable overheights calculated by different methods

ε	Numerical results of A_0	Eq. 14 A_0	Eq. 15 A_0	Eq. 16 A_0	Fourier series expansion	
					A_0	Error Eq. 17(%)
0·2	0·06604	0·07071	0·07042	0·07042	0·07042	$2·78 \times 10^{-6}$
0·4	0·13073	0·14142	0·13908	0·13914	0·139136	$2·78 \times 10^{-6}$
0·6	0·19280	0·21213	0·20422	0·20471	0·204652	$2·78 \times 10^{-6}$
0·8	0·25132	0·28284	0·26410	0·26615	0·265825	$2·78 \times 10^{-6}$
1·0	0·30565	0·35355	0·31694	0·32322	0·321942	$2·78 \times 10^{-6}$
1·2	0·35543	0·42426	0·36100	0·37661	0·372706	$2·79 \times 10^{-6}$
1·4	0·40067	0·49497	0·39451	0·42826	0·418164	$2·95 \times 10^{-6}$
1·6	0·44147				0·458607	$4·82 \times 10^{-6}$
1·8	0·47819				0·494473	$2·04 \times 10^{-5}$
2·0	0·51118				0·526263	$1·19 \times 10^{-4}$
2·2	0·54084				0·554482	$6·16 \times 10^{-4}$
2·4	0·56754				0·579605	$2·67 \times 10^{-3}$
2·6	0·59176				0·602059	$9·88 \times 10^{-3}$
2·8	0·61365				0·622213	$3·17 \times 10^{-2}$
3·0	0·63372				0·640387	$9·97 \times 10^{-2}$
3·2	0·65161				0·656850	0·23
3·4	0·66768				0·671846	0·53
3·6	0·68257				0·685611	1·08
3·8	0·70136				0·698525	2·10
4·0	0·71749				0·712472	4·76
4·2	0·72733				0·726384	16·83
4·4	0·74057				0·751754	13·79
4·6	0·74708				0·768796	17·09
4·8	0·75526				0·792551	31·40
5·0	0·76372				0·808718	23·25
5·2	0·77106				0·618304	499·64

by Callaghan and Nielsen [10]. In their numerical simulation, the domain length (in the *x*-direction) was sufficiently large for the local watertable fluctuation at the landward boundary to be negligible, replicating the condition of (2b). Although the simulation started with an initial condition ($h(x, 0) = 0$), it was run for a very long time to achieve a periodic solution. Results of previous analytical solutions (below) are also presented for comparison,

$$A_0 = \frac{\sqrt{2}}{4}\varepsilon + O\left(\varepsilon^3\right), \tag{14}$$

$$A_0 = \frac{\sqrt{2}}{4}\varepsilon + \frac{\sqrt{2} - 2}{16}\varepsilon^3 + O\left(\varepsilon^5\right), \tag{15}$$

$$A_0 = \frac{\sqrt{2}}{4}\varepsilon + \frac{\sqrt{2} - 2}{16}\varepsilon^3 + \frac{56 - 31\sqrt{2} + 24\sqrt{3} - 18\sqrt{6}}{1536}\varepsilon^5 + O\left(\varepsilon^7\right). \tag{16}$$

The new analytical solution, in its complete form ((6)–(13)), applies for $\varepsilon_0 > 1$ (i.e., $\varepsilon > \sqrt{2}$). In practical applications, the truncation of the series affects the accuracy of the solution. The solution is found to deteriorate when ε_0 is larger than 3·0 (i.e., $\varepsilon > 4·0$ with error $> 10\%$). Here the error is defined based on the matching of the boundary condition, i.e.,

$$\text{Error} = \max_{0 \leq T \leq 2\pi} |H\left[X_0\left(T\right), T\right] - \cos\left(T\right)|. \tag{17}$$

This error provides an indication of the solution's inaccuracy in predicting the watertable fluctuations (including but not just the watertable overheight). The error becomes increasingly large once $\varepsilon > 4·0$
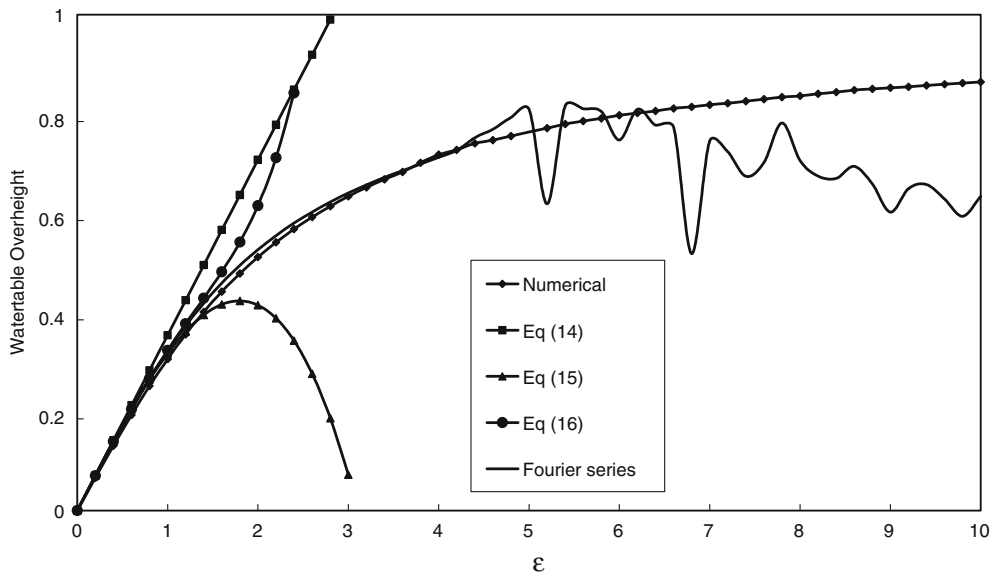
Fig. 2 Comparison of watertable overheights predicted by different methods

(Table 1) and cannot be reduced practically by including more terms of the series in the calculation. This is due to the numerical approximations in calculating the integrals for the Fourier coefficients and numerical solutions to the linear algebraic equations. Moreover, the adopted linear analytical formulation (6) with finite terms is inadequate for representing the actual nonlinear problem if ε gets larger than some critical value (in this case, 4·0).

The comparison of the predicted watertable overheight by different methods is also shown in Fig. 2. From both Table 1 and Fig. 2, it is evident that the predictions by the present analytical solution are very close to the numerical results, even for ε up to 5·0. The applicability of the solution, however, should be based on the match of the tidal boundary condition and constrained by $\varepsilon < 4·0$.

4 Asymptote of watertable overheight

In this section, we will prove that the asymptote of watertable overheight equals the tidal amplitude as ε approaches infinity. This result, obtained from numerical simulations reported previously by Callaghan and Nielsen [10], represents an extreme case of low-beach drainage conditions.

Making use of the property of the cosine function, we rewrite the Fourier coefficient $a_{n,2}(\varepsilon)$ as

$$a_{n,2}(\varepsilon) = \frac{1}{\pi} \int_0^{2\pi} f_n(\varepsilon, T) \cos(2T)\, \mathrm{d}T = 2a_{n,2}^*(\varepsilon) - a_{n,0}(\varepsilon), \tag{18}$$

where $a_{n,2}^*(\varepsilon) = \frac{1}{\pi} \int_0^{2\pi} f_n(\varepsilon, T) \cos^2(T)\, \mathrm{d}T$.

Below, we show that the following relationship holds

$$\lim_{\varepsilon \to \infty} a_{n,2}^*(\varepsilon) = - \lim_{\varepsilon \to \infty} a_{n,1}(\varepsilon). \tag{19}$$

For this purpose, we construct a new function

$$F_n(\varepsilon) = a_{n,2}^*(\varepsilon) + a_{n,1}(\varepsilon) = \int_0^{2\pi} f_n(\varepsilon, T) \cos(T)(\cos(T) + 1)\, \mathrm{d}T. \tag{20a}$$

Upon the application of integration rules, we have

$$F_n(\varepsilon) = 8 \int_0^{\pi/2} \exp\left(-\sqrt{2n}\varepsilon \cos^2(\tau)\right) \cos(2n\tau) \cos\left(\sqrt{2n}\varepsilon \cos^2(\tau)\right) \cos(2\tau) \cos^2(\tau) \, d\tau. \tag{20b}$$

Noting that the function $x \exp(-\sqrt{2n}\varepsilon x)$ has the maximum value $\frac{1}{e\sqrt{2n}\varepsilon}$ at $x = \frac{1}{\sqrt{2n}\varepsilon}$ in the interval $[0, 1]$, one can show

$$|F_n(\varepsilon)| \le \frac{4\pi}{e\sqrt{2n}\varepsilon}. \tag{21}$$

This yields

$$\lim_{\varepsilon \to \infty} F_n(\varepsilon) = 0, \tag{22}$$

and the maximum of function $f_n(\varepsilon, T) \cos(T)$ is $(-1)^{n+1}$ at $T = \pi$, which implies that $\lim_{\varepsilon \to \infty} a_{n,1}(\varepsilon)$ exists and satisfies Eq. 19.

From (18), we have

$$\lim_{\varepsilon \to \infty} a_{n,2}(\varepsilon) = -2 \lim_{\varepsilon \to \infty} a_{n,1}(\varepsilon) - \lim_{\varepsilon \to \infty} a_{n,0}(\varepsilon). \tag{23}$$

Similarly, we have the following result for $c_{n,2}(\varepsilon)$

$$\lim_{\varepsilon \to \infty} c_{n,2}(\varepsilon) = -2 \lim_{\varepsilon \to \infty} c_{n,1}(\varepsilon) - \lim_{\varepsilon \to \infty} c_{n,0}(\varepsilon). \tag{24}$$

Using (12) with $l = 1$ and $l = 2$ in conjunction with (23) and (24), we have

$$\lim_{\varepsilon \to \infty} \sum_{n=1}^{\infty} \left(a_{n,0}(\varepsilon) A_n + c_{n,0}(\varepsilon) B_n\right) = -2 \lim_{\varepsilon \to \infty} \sum_{n=1}^{\infty} \left(a_{n,1}(\varepsilon) A_n(\varepsilon) + c_{n,1}(\varepsilon) B_n(\varepsilon)\right) = -2. \tag{25}$$

Based on (11) and (25), one can determine the limit of $A_0(\varepsilon)$ (the watertable overheight normalised by the tidal amplitude)

$$\lim_{\varepsilon \to \infty} A_0(\varepsilon) = -\frac{1}{2} \lim_{\varepsilon \to \infty} \sum_{n=1}^{\infty} \left(a_{n,0}(\varepsilon) A_n(\varepsilon) + c_{n,0}(\varepsilon) B_n(\varepsilon)\right) = 1. \tag{26}$$

5 Conclusions

In this note we have presented a new approach to solving the linearised one-dimensional Boussinesq equation subject to tide-induced moving-boundary conditions. The technique, which is based on Fourier series, allows analytical predictions of tidal watertable overheight in coastal aquifers of low hydraulic diffusivity and small beach slope. The analytical solution applies for $\varepsilon_0 > 1$ in theory but is limited by $\varepsilon_0 < 3.0$ in practical applications. This solution extends previous perturbation solutions based on $\varepsilon_0 < 1$. Moreover, based on the new approach we prove that the asymptote of watertable overheight, as ε_0 approaches infinity, equals the tidal amplitude, a result obtained only numerically in previous studies.

Based on the results presented in this paper, further studies may be carried out to (i) improve the accuracy of the numerical approximations in calculating the integrals for the Fourier coefficients and numerical solutions to the linear algebraic equations; (ii) seek a mathematical function of the groundwater tidal overheight for $0 \le \varepsilon < \infty$; and (iii) study the dynamical characteristics of the tidal watertable with different values of ε.

References

1. Philip JR (1973) Periodic nonlinear diffusion: an integral relation and its physical consequences. Aust J Phys 26:513–519
2. Parlange JY, Stagnitti F, Starr JL, Braddock RD (1984) Free-surface flow in porous media and periodic solution of the shallow-flow approximation. J Hydrol 70:251–263
3. Nielsen P (1990) Tidal dynamics of the water table in beaches. Water Resour Res 26:2127–2134
4. Li L, Barry DA, Stagnitti F, Parlange JY, Jeng DS (2000) Beach water table fluctuations due to spring-neap tides: moving boundary effects. Adv Water Resour 23:817–824
5. Simmons GM (1992) Importance of submarine groundwater discharge and sea water cycling to material flux across sediment/water interfaces in marine environments. Mar Ecol Prog Ser 84:173–184
6. Church TM (1996) A groundwater route for the water cycle. Nature 380:579–580
7. Moore WS (1996) Large groundwater inputs to coastal waters revealed by [226]Ra enrichment. Nature 380: 612–614
8. Li L, Barry DA, Stagnitti F, Parlange JY (1999) Submarine groundwater discharge and associated chemical input to a coastal sea. Water Resour Res 35:3253–3259
9. Li HL, Jiao JJ (2003) Tide-induced seawater-groundwater circulation in a multi-layer coastal leaky aquifer system. J Hydrol 274:211–224
10. Callaghan D, Nielsen P (accepted) A note on the theoretical rise in mean groundwater elevation for very flat beaches driven solely by the tide. Adv Water Resour
11. Bear J (1972) Dynamics of fluids in porous media. Amsterdam Elsevier, New York
12. Harris JW, Stocker H (1998) Handbook of mathematics and computational science. Springer-Verlag, New York